



# Thermal Analysis of Self-Propagating Reaction Joining Material

by Luna H. Chiu, Dennis C. Nagle,  
Daniel J. Snoha, and Kyu Cho

ARL-TR-1906

March 1999

19990325 052

Approved for public release; distribution is unlimited.

The findings in this report are not to be construed as an official Department of the Army position unless so designated by other authorized documents.

Citation of manufacturer's or trade names does not constitute an official endorsement or approval of the use thereof.

Destroy this report when it is no longer needed. Do not return it to the originator.

# **Army Research Laboratory**

Aberdeen Proving Ground, MD 21005-5069

---

**ARL-TR-1906****March 1999**

---

## **Thermal Analysis of Self-Propagating Reaction Joining Material**

**Luna H. Chiu, Daniel J. Snoha, and Kyu Cho**  
Weapons and Materials Research Directorate, ARL

**Dennis C. Nagle**  
Johns Hopkins University

---

## Abstract

---

This report focuses on the characterization of self-propagating high-temperature synthesis (SHS) reactions that occur in powder compacts containing titanium, boron, and aluminum. Interest in this powder system is based on the critical need to develop new joining techniques for bonding ceramics to metals. The exothermic reactions of particular interest in this study include those that generate  $\text{TiB}_2$ ,  $\text{TiB}$ ,  $\text{Ti}_3\text{Al}$ , and  $\text{TiAl}$  from their elemental powders. Data from differential thermal analysis, thermogravimetric analysis, and x-ray diffractometry are presented. These results demonstrate that the gas phase surrounding the SHS powders plays an important role in initiating the SHS reaction and in determining which reaction products will form in the final bond.

# Table of Contents

	<u>Page</u>
<b>List of Figures .....</b>	<b>v</b>
<b>List of Tables.....</b>	<b>v</b>
<b>1. Introduction .....</b>	<b>1</b>
<b>2. Experimental.....</b>	<b>3</b>
2.1 Powder Characterization and Preparation .....	3
2.2 Thermal Analysis.....	4
2.3 X-ray Diffraction.....	4
<b>3. Results and Discussion.....</b>	<b>5</b>
3.1 Powder Characterization .....	5
3.2 Thermal Analysis of Starting Powders .....	6
3.3 Two Component Reactions .....	10
3.4 Three Component Reactions.....	14
<b>4. Conclusions .....</b>	<b>17</b>
<b>5. References .....</b>	<b>21</b>
<b>Distribution List.....</b>	<b>23</b>
<b>Report Documentation Page.....</b>	<b>25</b>

INTENTIONALLY LEFT BLANK.

## List of Figures

<u>Figure</u>	<u>Page</u>
1. DTA/TGA Results vs. Temperature of Pure Titanium Heated in Air and Argon .....	7
2. DTA of Titanium Heated in Argon From 700° C to 1,000° C .....	7
3. DTA/TGA Results vs. Time for Titanium Heated in Air .....	8
4. DTA/TGA Results for Aluminum Heated in Air and Argon .....	9
5. DTA/TGA Results for Amorphous Boron Heated in Air and Argon .....	9
6. DTA/TGA Results of Ti + Al → TiAl Reacted in Air and Argon .....	10
7. DTA/TGA of Ti + Al → TiAl Reacted in Argon From 600° C to 900° C .....	11
8. X-ray Diffraction of Ti + Al Reacted in Argon .....	11
9. X-ray Diffraction of Ti + Al Reacted in Air .....	12
10. DTA/TGA Results of Ti + 2B Reacted in Air and Argon .....	15
11. X-ray Diffraction for Ti + 2B Reacted in Argon .....	15
12. X-ray Diffraction for Ti + 2B Reacted in Air .....	16
13. DTA/TGA Results of 50% by Weight Al + 50% (Ti + 2B) Reacted in Air .....	16
14. X-ray Diffraction of 50% by Weight Al + 50% (Ti + 2B) Reacted in Air .....	17
15. X-ray Diffraction of 50% by Weight Al + 50% (Ti + 2B) Reacted in Argon .....	18

## List of Tables

<u>Table</u>	<u>Page</u>
1. Summary of Powder Size and Surface Area .....	5

INTENTIONALLY LEFT BLANK.



# 1. Introduction

For optimum performance of many aerospace, commercial, and military systems, the use of dissimilar materials is becoming increasingly necessary [1, 2]. Therefore, the joining of advanced materials, composites, and ceramics to metal structures is a prominent issue [3]. Joining ceramics to metals presents a particularly difficult task due to the differences in mechanical and thermal properties of these materials. These differences can lead to excessive stress at the joining interfaces, causing mechanical failure in the form of microcracks [4]. Current techniques for joining these advanced materials include the use of polymer-based adhesion, mechanical fastening, and welding. In general, polymeric adhesives do not enhance the overall performance of the structure. Also, commercially available polymeric adhesives will degrade at temperatures higher than 180° C [5]. This severely limits the applications in which polymeric adhesives can be used. Mechanical fasteners, such as bolts and sleeves, concentrate stresses and increase the chances of brittle fracture and, ultimately, failure of the ceramic part. To alleviate these problems, ceramic parts are often metallized, which adds steps in the manufacturing process and increases the total cost of the component [6]. Also, parts must be designed to distribute stresses resulting from mechanical fastening as homogeneously as possible. Welding, on the other hand, often results in oxidization and/or recrystallization of the metal, especially when a repair is performed. Many welding filler metals do not wet ceramic components. Differences in thermal expansion of the weld filler and substrate can also lead to bond failure [6]. Further, specially trained welders are usually needed, which adds to the cost of joining.

The ultimate goal of this research is to investigate the joining of ceramics to metals by self-propagating high-temperature synthesis (SHS) reactions. Thermite reactions involving metal-oxide reactions have been used for many decades to join steel structures [7]. In contrast to thermite reactions, the SHS reactions are primarily used to produce refractory metal compounds and ceramics from compacted mixtures of elemental powders [8, 9]. Like thermite reactions, SHS reactions are typically initiated by heating a small portion of the powder compact with a hot filament or flame. Once initiated, the exothermic heat is sufficient to propagate the reaction throughout the mixture. The main advantage of using this method for joining is the generation of high temperatures (1,200–4,000° C) [10] for short periods of time, which minimizes the heat-affected zone in the metal.

The very high heat of the SHS reaction can also desorb the impurities physically adsorbed on the powder surfaces [11]. This method offers the potential for the field bonding of components at a relatively low cost, since these bond joints can be made with almost no capital equipment. Many of these reactions can be initiated by a 12-V battery and usually require no special training.

The SHS reactions investigated in this study are similar to SHS processes described in Nagle, Brupbacher, and Christodoulou [12] for formation of discontinuous metal matrix composites where ceramic reinforcements are formed *in situ* in a host metal matrix. Moshier et al. [13] in their patent reveal a method for bonding metals and metal matrix composites to other metal-based materials by welding with filler materials that are metal matrix composites generated by SHS. In contrast, the goal of this research is to utilize the heat generated from the SHS process to bond dissimilar materials *in situ*, while forming the metal matrix composite that is the bond material.

The materials to be bonded are alumina ceramic ( $\text{Al}_2\text{O}_3$ ) and titanium metal. The SHS system chosen to form the bond is the combination of titanium, aluminum, and boron powders. The SHS reaction of these powders results in  $\text{TiB}_2$  precipitating in a matrix of  $\text{TiAl}$ ,  $\text{Ti}_3\text{Al}$ , or  $\text{Al}$ . The concept for bonding is that these powders would be pressed into a green compact and sandwiched between the ceramic (alumina) and metal (titanium). This compact would then be ignited and reacted. Currently, it is believed that the SHS reactions in the Ti-Al-B system are initiated by the melting of the aluminum metal. Subsequently, a portion of the titanium and boron powders dissolve and react to form  $\text{TiB}_2$ , which precipitates from the melt [14, 15]. Temperatures in excess of  $3,000^\circ\text{C}$  are generated by these reactions. Under optimal conditions, the heat produced by this reaction would melt the surface of the metallic component to be joined. Due to this melting, a metallurgical bond would form with the metal component. A mechanical bond would form with the ceramic where molten metal wets the ceramic and wicks into the pores. Using this approach for bonding metals and ceramics, the joint formed by a ceramic particulate dispersed in a metal matrix would have properties intermediate between those of the ceramic and of the metal, based on a rule of mixtures. This type of material would decrease the stress localized at the interface and distribute the stresses throughout the bond.

The focus of the present investigation is to gain a better understanding of the reactions between the SHS components and the effects of the presence or absence of oxygen on the reactions. Where possible, the mechanisms associated with the formation of the final products are addressed. This report presents thermal analysis studies in air and argon of titanium, aluminum, and boron powders, individually and in combination. The results of this study will be used to select parameters for SHS bonding.

## 2. Experimental

All the starting elemental powders were characterized for surface area, particle size, morphology, crystallinity, and purity. The effects of atmosphere on the exothermic reaction were studied by simultaneous differential thermal analysis (DTA) and thermogravimetric analysis (TGA) in air and in argon on three sets of powder mixes. The first set of experiments encompassed thermal analysis of the elemental powders of titanium, boron, and aluminum individually. A second set of thermal data was obtained for the two binary reactions of the elemental powders. These reactions are  $\text{Ti} + \text{Al} \rightarrow \text{TiAl}$  and  $\text{Ti} + 2\text{B} \rightarrow \text{TiB}_2$ . Finally, reactions of all three of the elemental powders were studied. The composition of primary interest was 50% by weight of aluminum mixed with 50% of  $(\text{Ti} + 2\text{B})$ . To interpret many of the thermal analysis results, powder x-ray diffraction analysis was performed on all of the unreacted powders and their SHS reaction products.

**2.1. Powder Characterization and Preparation.** All of the elemental powders were obtained from the Alpha Aesar company. The powder specifications are as follows: titanium powder, -325 mesh, 99% (metals basis); aluminum powder, -325 mesh, 99.5% (metals basis); amorphous boron powder, -325 mesh, 99.99% (metals basis). The "as-received" metal powders were opened under argon to minimize their exposure to air and moisture. This also reduced the potential for dust explosions, since many fine metal powders can be pyrophoric.

The particle size of the titanium and aluminum powder was obtained using a Micromeritics 5100 sedigraph, which uses an x-ray scattering technique. Prior to particle size measurement, the

metal powders were dispersed in ethanol and mixed using an ultrasonic probe. This technique can only be used for particles with an atomic number greater than that of carbon. Thus, the particle size of the amorphous boron powder was obtained using Photo Correlation Spectra (PCS), which is a dynamic light scattering method. The boron powder was suspended in water using an ultrasonic probe prior to being placed in the PCS chamber. The surface area data were obtained using a Coulter SA3100 Brunauer, Emmett, and Teller (BET) apparatus. Scanning electron microscopy (SEM) and transmission electron microscopy (TEM) techniques were used to characterize the morphology of the powders. Finally, powder x-ray diffraction analysis was performed on the Ti, Al, and amorphous B powders to check for crystallinity and gross impurities. When the elemental powders were mixed, the correct atomic ratios were placed in small Nalgene bottles under argon in quantities of 5 g of total powder. The powders were mixed by stirring with stainless steel instruments. The powders were also mixed for 10 min just prior to thermal SHS reaction.

**2.2. Thermal Analysis.** Simultaneous DTA/TGA analysis was performed using a TA Instruments model 2960, capable of reaching a maximum temperature of 1,500° C. Two series of experiments were performed using the elemental Ti, Al, and B powders. One series was reacted in an argon atmosphere and a second set with a bottled air atmosphere, where composition of the bottled air was 80% N<sub>2</sub> + 20% O<sub>2</sub>. A similar set of experiments was performed to characterize the reactions involving  $\text{Ti} + \text{Al} \rightarrow \text{TiAl}$  and  $\text{Ti} + 2\text{B} \rightarrow \text{TiB}_2$ . Again, each reaction was investigated to determine the role of atmospheric oxygen on the reaction and the subsequent reaction products. Finally, thermal SHS experiments were performed on the mixture of 50% by weight Al + 50% (Ti + 2B) in argon and air atmospheres.

The DTA/TGA crucible volume was 90  $\mu\text{liters}$ . In all cases, the flow rate of each gas was 0.1 liters/min. The reference material used for the DTA/TGA was 99.99% pure Al<sub>2</sub>O<sub>3</sub> powder. The heating rate for all experiments was set at 50° C/min. Data were obtained from room temperature to 1,000° C.

**2.3. X-ray Diffraction.** In order to obtain a larger quantity of reacted powder for x-ray diffraction, powders were reacted in a tube furnace under the same conditions used for the DTA/TGA

thermal analysis. With each sample in the center of the tube, the appropriate gas was introduced at one end of the tube and passed through to the other end. The temperature in the tube furnace was increased at a rate of  $50^{\circ}\text{C}/\text{min}$  from room temperature to  $1,000^{\circ}\text{C}$ .

X-ray analyses were performed on the products of the binary and ternary reactions in air and argon. The reaction products were crushed to fine powders for the x-ray diffraction analysis.

### 3. Results and Discussion

**3.1. Powder Characterization.** Table 1 presents the particle size data for titanium, aluminum, and the amorphous boron powders obtained using the Micromeritics 5100 sedigraph and the photocorrelation spectrometer. The sedigraph result for the titanium powder showed a bimodal distribution with the main distribution between 10 and 60  $\mu\text{m}$  and a median diameter of 23.54  $\mu\text{m}$ . Approximately 10% of the particles were between 1  $\mu\text{m}$  and 10  $\mu\text{m}$  in size, with the median diameter being approximately 2  $\mu\text{m}$ . Calculations of surface areas using a weighted average of these two mean particle diameters yield a surface of  $0.12\text{ m}^2/\text{g}$ , which is in reasonable agreement with the measured surface area of  $0.34\text{ m}^2/\text{g}$  from BET data.

**Table 1. Summary of Powder Size and Surface Area**

Powder	Median Diameter ( $\mu\text{m}$ )	Surface Area ( $\text{m}^2/\text{g}$ )
Titanium	23.54	0.34
Aluminum	4.52	0.89
Boron	0.180	40.4

In the aluminum sample, the distribution had only one mode with a median diameter of 4.52  $\mu\text{m}$  present, and a particle size range between 1 and 15  $\mu\text{m}$  in size.

The amorphous boron powders had a very tight distribution, 0.164  $\mu\text{m}$ –0.232  $\mu\text{m}$ , with a mean diameter of 0.180  $\mu\text{m}$ . The mean particle diameter for all the powders used in this study is presented in Table 1, along with the BET surface area data.

SEM micrographs showed that the starting powders are very angular in shape for both the titanium and aluminum. The boron powder was imaged by TEM because the resolution of these small powders by SEM was not acceptable. The average powder size of the boron, based on the TEM results, was in agreement with the PCS data. The powder sizes are all in good agreement with the particle size data, as well as sizes relative to each other. The titanium was visibly larger than the aluminum and boron.

X-ray powder diffraction was performed on the powders to check for any gross impurities and to evaluate the crystallinity of the powders. The titanium and aluminum were confirmed to be pure with very sharp peaks. The boron was amorphous with no visible signs of crystalline peaks.

**3.2. Thermal Analysis of Starting Powders.** The first set of experiments involved the thermal analysis of all the starting powders. These thermal experiments were conducted in both air and argon. Figure 1 is the DTA/TGA data for titanium powder heated in air and argon. When an argon atmosphere was employed, the titanium powder was thermally stable, showing only a minimal weight gain above 700° C; this weight gain was probably due to residual oxygen in the furnace chamber. Figure 2 shows a closeup of the DTA of titanium in argon between 700–1,000° C. The titanium phase transition from hexagonal close packed (HCP) to body-centered cubic (BCC) was detected at 880° C from this DTA data.

When Ti was heated in air, two exotherms were observed, one with an onset around 520° C and another at 700° C. When the TGA is graphed against time (Figure 3), it can be seen that the weight gain for each exotherm is linear with time and there are two distinct slopes; this fact suggests the formation of two different products, which were certainly titanium oxides. By visual inspection, the sample had three distinct layers. The outer surface was yellow, the next layer white, and the bottom layer metallic gray. It is known that  $\text{TiO}$  is yellow,  $\text{TiO}_2$  is white, and Ti is metallic gray in color [16].

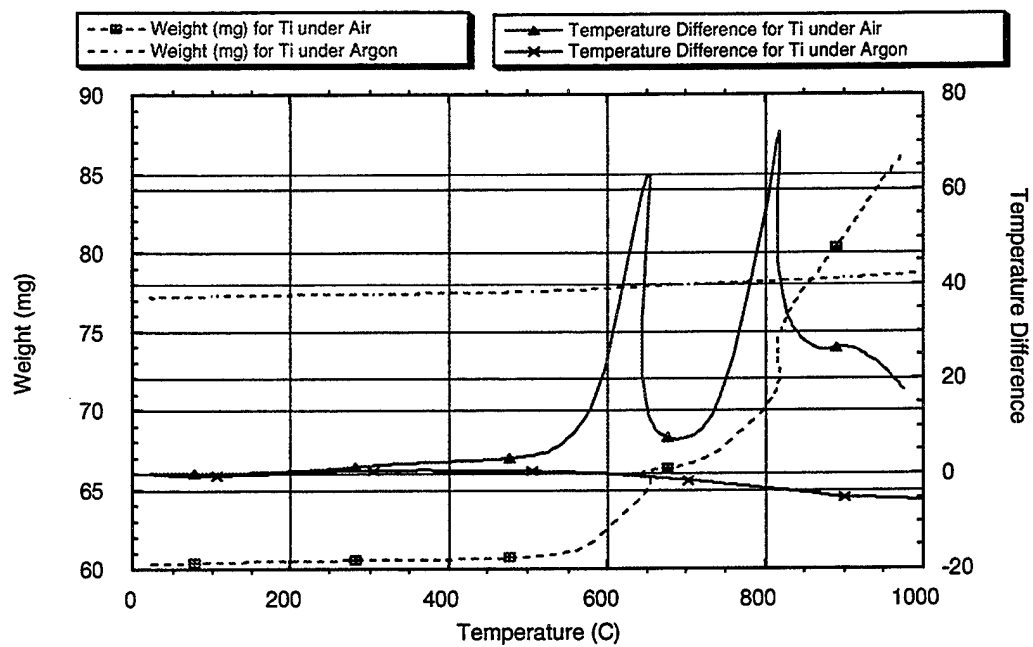


Figure 1. DTA/TGA Results vs. Temperature of Pure Titanium Heated in Air and Argon.

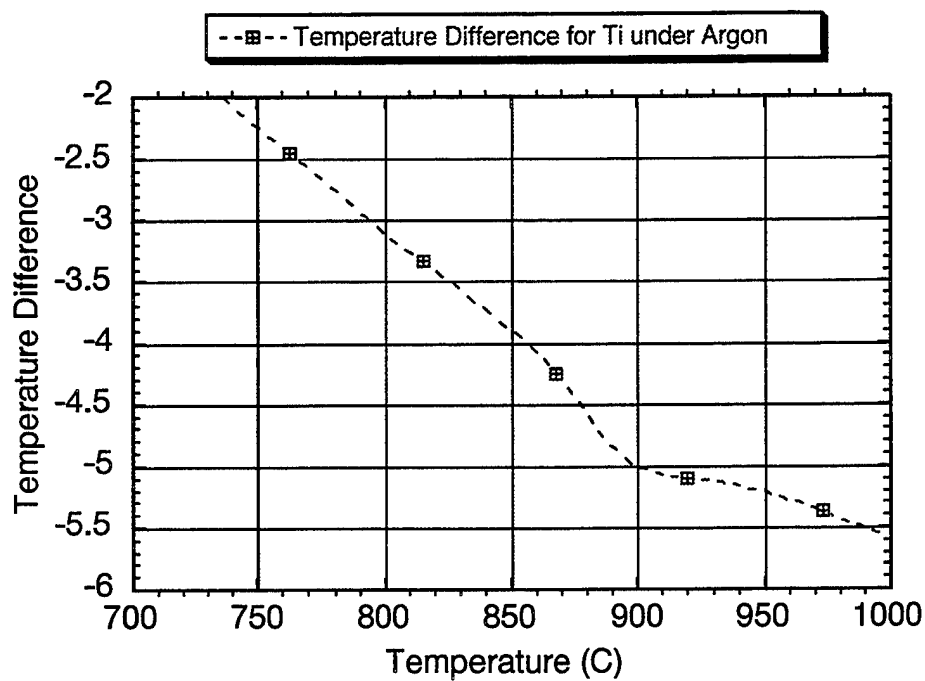
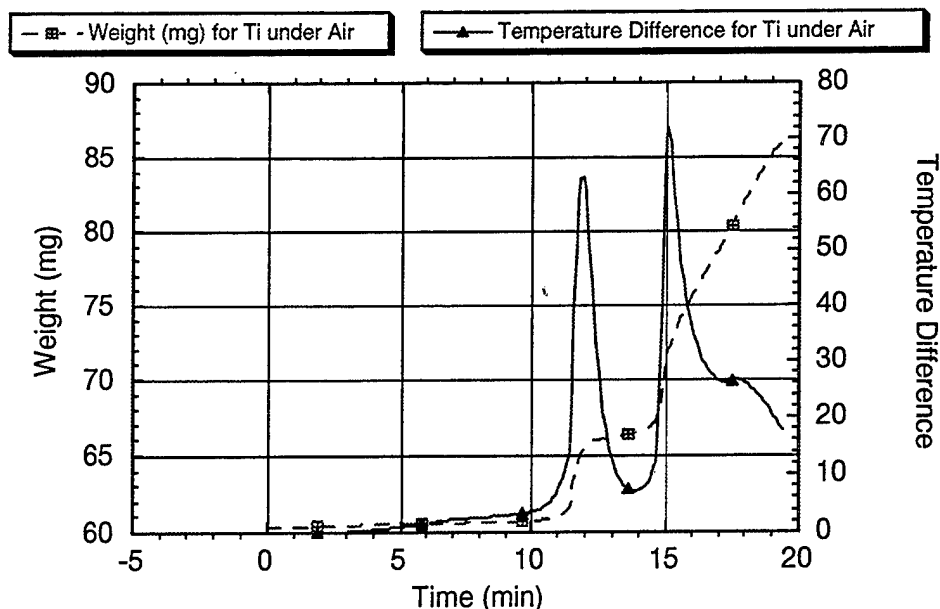


Figure 2. DTA of Titanium Heated in Argon from 700° C to 1,000° C.



**Figure 3. DTA/TGA Results vs. Time for Titanium Heated in Air.**

Figure 4 shows the thermal results for the pure aluminum sample heated in argon and air. The data in argon show the aluminum melting endotherm with an onset temperature around  $660^{\circ}\text{C}$ , and the associated TGA results showed no significant weight gain.

Note that  $660^{\circ}\text{C}$  is the melting point of aluminum. For the aluminum sample heated in air, an exotherm starts at  $620^{\circ}\text{C}$  and an associated weight gain of approximately 4% is observed. This is interpreted as rapid oxidation of the aluminum beginning at  $620^{\circ}\text{C}$ . From the DTA data, it appears that the remaining material starts to melt at  $660^{\circ}\text{C}$ , as indicated by the sharp decrease of the DTA trace and even a slight endotherm at this temperature. Note that the weight plateaued at this point and then increased more rapidly above  $750^{\circ}\text{C}$ . It is presumed that, because of the higher coefficient of thermal expansion of the molten aluminum, the aluminum oxide layer formed at  $620^{\circ}\text{C}$  cracks and the combination of this effect and the enhanced oxygen diffusion at the higher temperature allows the oxidation process to proceed.

Figure 5 presents the DTA and TGA data for the heating of boron in air and argon. The boron heated under argon did not have any significant reactions or phase changes in the inert atmosphere



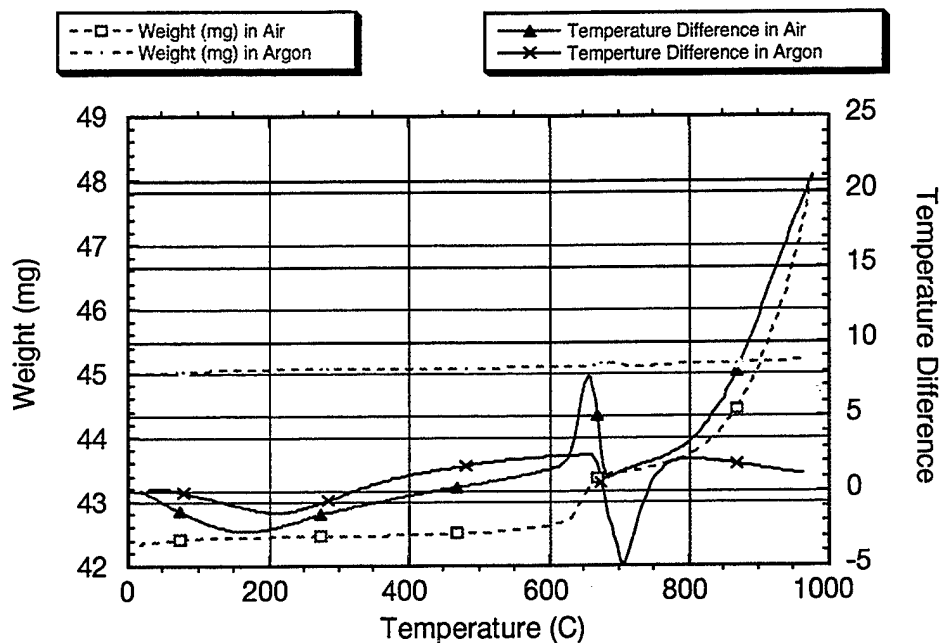


Figure 4. DTA/TGA Results for Aluminum Heated in Air and Argon.

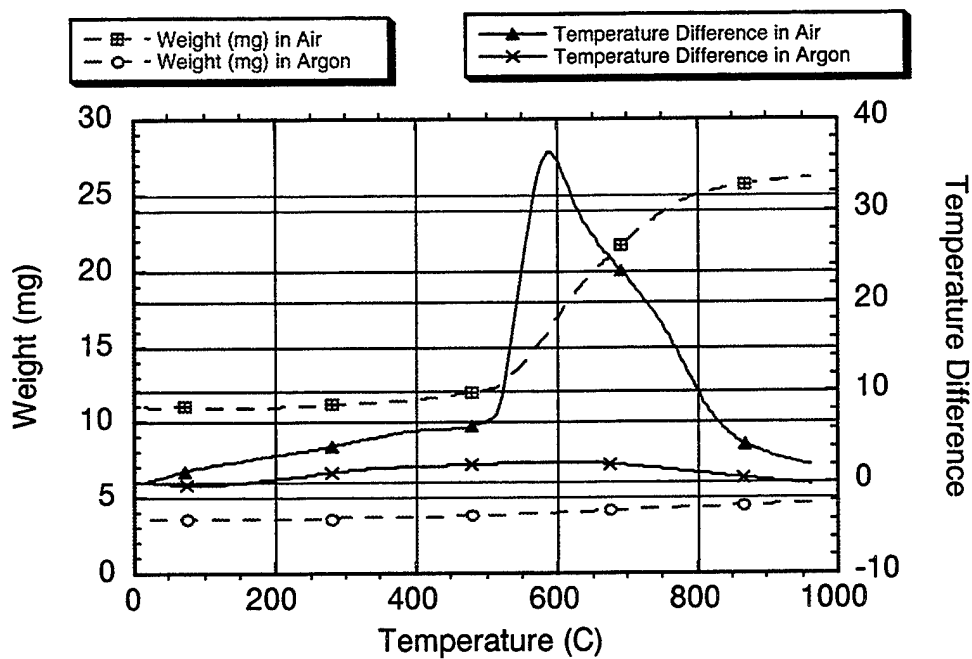
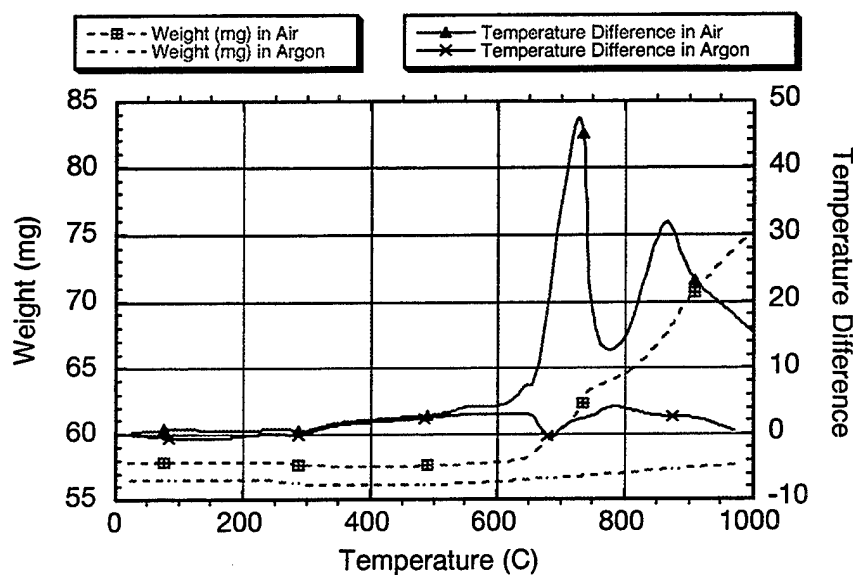


Figure 5. DTA/TGA Results for Amorphous Boron Heated in Air and Argon.

from room temperature to 1,000° C. However, when the same powder was heated in air, there was a very apparent exotherm found to start at 520° C. This fact, along with the increase in weight, indicated that the boron started oxidizing at this temperature and continued to oxidize up to 800° C.

**3.3 Two Component Reactions.** The thermal analysis results for the reaction of titanium and aluminum in argon and air is shown in Figure 6. The DTA result for the two components heated in argon showed an endotherm starting at 660° C; this endotherm correlates to the temperature at which aluminum melts. This endotherm is followed by an exotherm, seen more clearly in Figure 7, and is most likely related to the formation of bulk TiAl, as well as Ti<sub>3</sub>Al. Both of these reactions are exothermic [17].



**Figure 6. DTA/TGA Results of Ti + Al  $\rightarrow$  TiAl Reacted in Air and Argon.**

The complementary x-ray diffraction (XRD) patterns confirmed the formation of both titanium aluminides (Figure 8). The melting of the aluminum at 660° C allowed for greater surface contact of the components, increased diffusion, and should therefore decrease the energy required for intermetallic formation. The phenomena of SHS reactions occurring more readily in a liquid-solid as opposed to solid-solid systems is well documented [11, 17, 18].

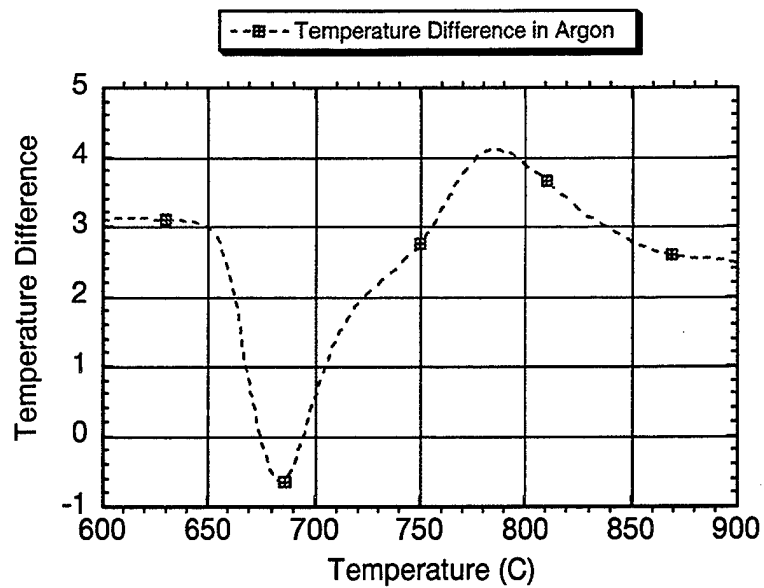


Figure 7. DTA/TGA of Ti + Al  $\rightarrow$  TiAl Reacted in Argon From 600° C to 900° C.

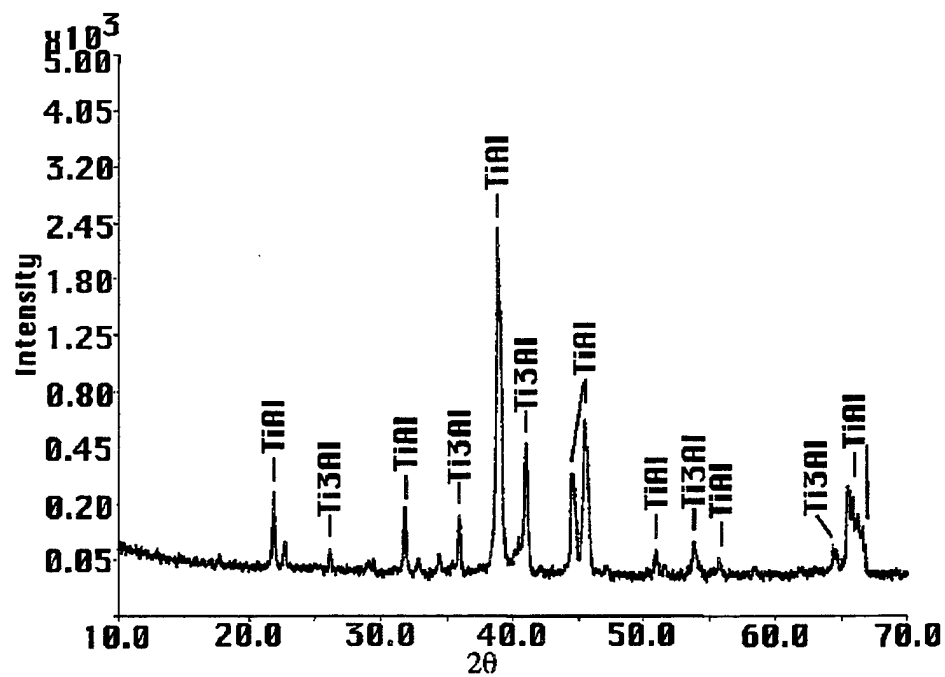


Figure 8. X-ray Diffraction of Ti + Al Reacted in Argon.

When the titanium and aluminum were heated in air, the DTA results showed two distinct exotherms, the first starting at 620° C and a second starting at 775° C. These two exotherms resemble the curve for titanium heated in air (see Figure 1). These exotherms are due to both the formation of intermetallic compounds, as well as metal oxidation, based upon the XRD data (Figure 9). It is difficult to label which of the exotherms is related to which products, since all reactions are exothermic. Comparison of the areas under the 620° C exotherms indicates that more heat was generated from the Ti + Al reaction than from the pure titanium in air (see Figure 1).

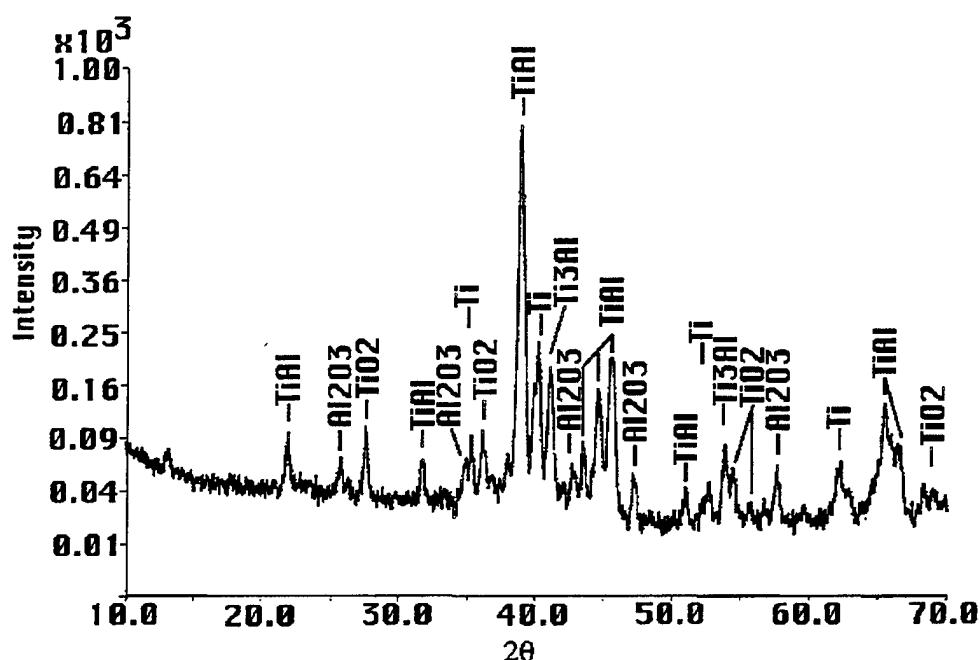


Figure 9. X-ray Diffraction of Ti + Al Reacted in Air.

The amount of heat produced by each reaction was calculated from the area under the DTA curve by using equations (1), (2), and (3) [19, 20].

The DTA apparatus was first calibrated using known substances, and a calibration constant was determined for the experimental conditions by equations (1) and (2).

$$E_L = \frac{(H_L * m_L)}{A_L} \quad E_H = \frac{(H_H * m_H)}{A_H} \quad (1)$$

$$E_x = (T_x - T_L) * \frac{(E_H - E_L)}{(T_H - T_L)} + E_L \quad (2)$$

$$H_x = \frac{(E_x A_x)}{m_x}, \quad (3)$$

where

$E_L$  = calibration constant for a calibration material with lower melting temperature

$E_H$  = calibration constant for a calibration material with higher melting temperature

$E_x$  = calibration constant for material in question

$T_L$  = peak temperature for calibration material with lower melting temperature

$T_H$  = peak temperature for calibration material with higher melting temperature

$H_L$  = known heat for lower melting point calibration material

$H_H$  = known heat for higher melting point calibration material

$H_x$  = heat produced by material in question

$m_L$  = mass of lower melting calibration specimen

$m_H$  = mass of higher melting calibration specimen

$m_x$  = mass of material in question

$A_L$  = area under curve of lower melting calibration material

$A_H$  = area under curve of higher melting calibration material

$A_x$  = area under curve of the DTA in question

When these calculations are performed using pure aluminum as the low-temperature calibration material and sodium chloride as the high-temperature calibration material, the heat generated by the first exotherm of Ti + Al is measured to be 30% greater than the heat generated by the first exotherm in titanium. It is noted that pure aluminum also produces a small exotherm at 620° C; however, the

heat produced was relatively small. The extra 30% heat was surely due to the reaction that formed the intermetallics. The 775° C exotherm is also a combination of oxide and intermetallic formation, with the majority of the heat produced by the intermetallics, which was the major phase formed.

Based on the thermal and XRD results, it is believed that the catalytic heat was added to the system by oxidation of the components; this heat, along with the ambient temperature at that time, allowed the initiation of the intermetallic reaction.

Figure 10 shows the DTA/TGA results for Ti + 2B reacted in air and argon. The sample that was reacted in argon showed no prominent features. The behavior was very similar to that of pure boron heated in argon. There was no melting of any of the constituents. The x-ray results of Ti + 2B heated in argon showed the major phase as the unreacted titanium. The boron was amorphous and did not show up in the pattern; however, a small amount of TiB<sub>2</sub> and TiB was detected (Figure 11). Since there was no exotherm detected, the formation of TiB<sub>2</sub> and TiB was due to solid-state diffusion rather than a SHS-type phenomenon.

When the Ti + 2B was reacted in air, oxidation started to occur at 500° C. This curve is very similar to that of pure boron reacted in air. Using the calculations for heat produced shows that the heat produced in this reaction is slightly greater than just for the boron oxidation. The extra heat generated was produced by titanium oxidation and TiB<sub>2</sub> formation, as is evidenced by the XRD results (Figure 12).

**3.4. Three Component Reactions.** The primary candidate composition for SHS bond joint materials is 50% by weight Al + 50% (Ti + 2B). DTA/TGA measurements for this composition were performed in air and argon (Figure 13). When the composition was reacted in an oxygenated atmosphere, there was a large exotherm produced, which was expected based on the previous data. This exotherm started at the same temperature as the start of pure titanium oxidation. The boron was also expected to oxidize before the melting point of aluminum; however, XRD results confirmed TiO<sub>2</sub> as the only oxide present (Figure 14). It is believed that the titanium reacts with the oxygen in the

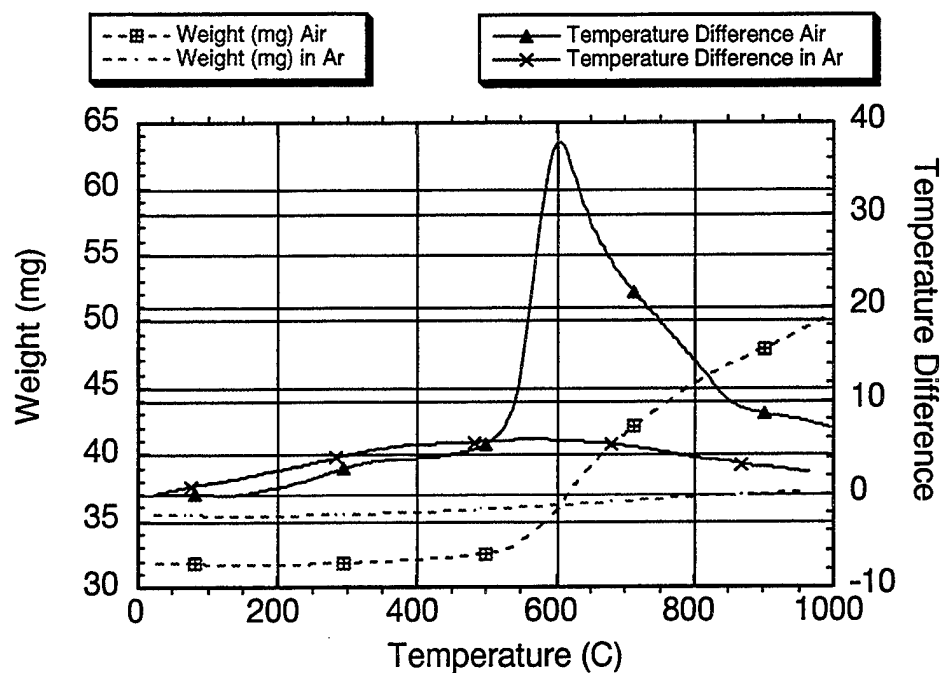


Figure 10. DTA/TGA Results of Ti + 2B Reacted in Air and Argon.

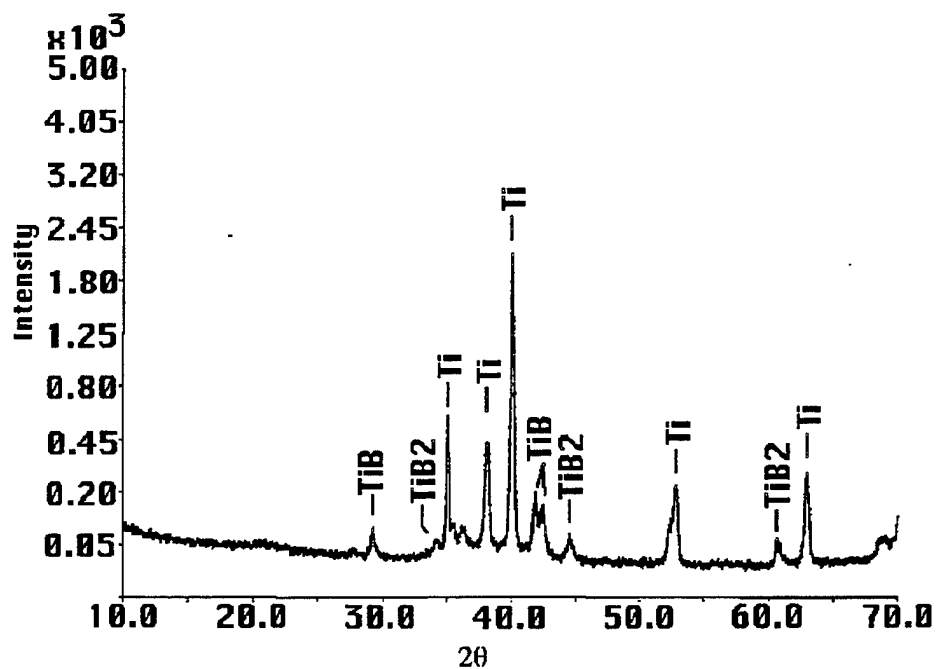


Figure 11. X-ray Diffraction for Ti + 2B Reacted in Argon.

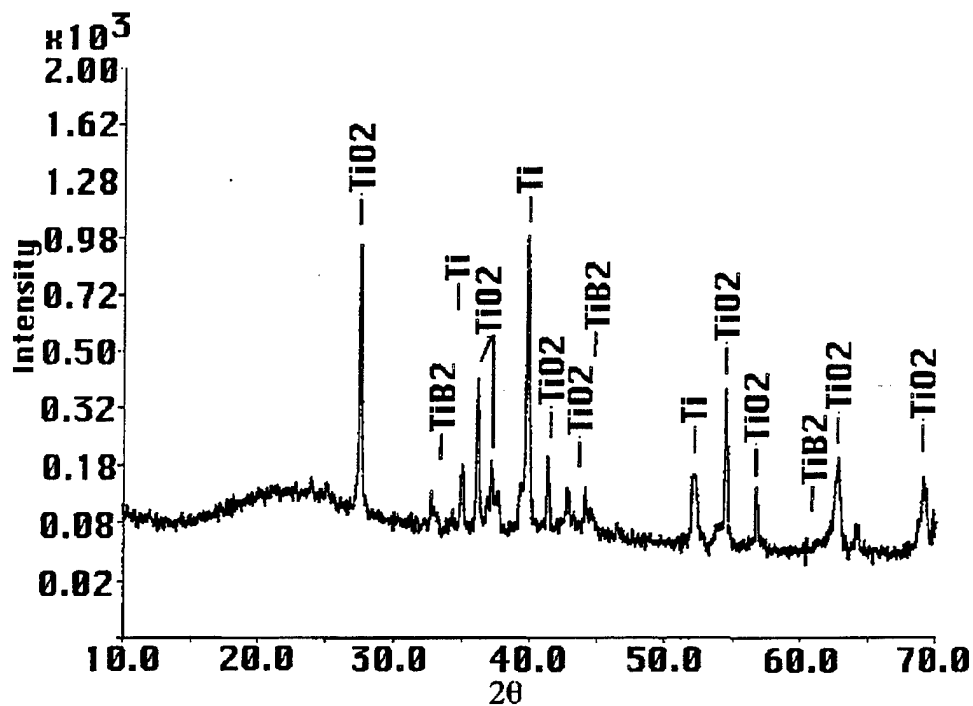


Figure 12. X-ray Diffraction for Ti + 2B Reacted in Air.

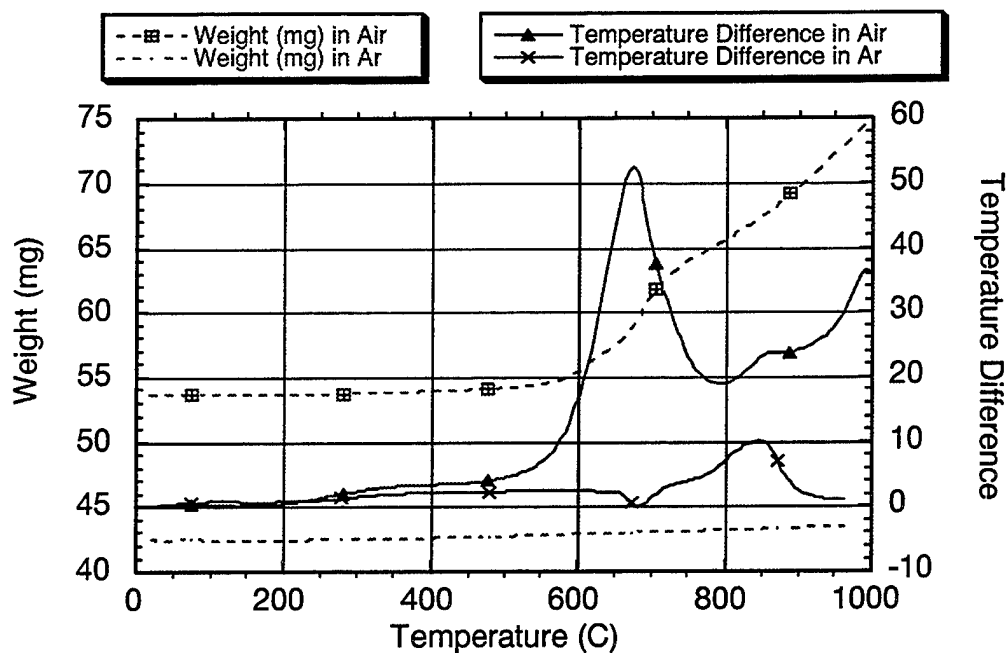


Figure 13. DTA/TGA Results of 50% by Weight Al + 50% (Ti + 2B) Reacted in Air.



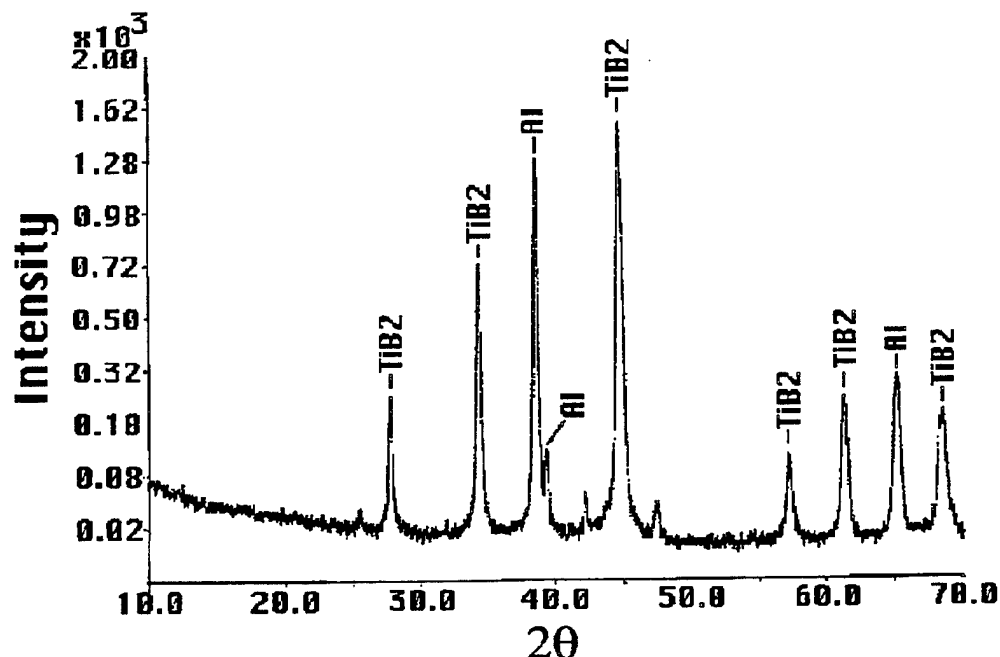


Figure 14. X-ray Diffraction of 50% by Weight Al + 50% (Ti + 2B) Reacted in Air.

system and produces enough heat to start the SHS reaction of  $\text{TiB}_2$  formation. The reason for this is that the exothermic peak starts prior to aluminum melting temperature. Also  $\text{TiO}_2$  was only a residual phase found in the XRD analysis; the majority of the heat produced was probably generated by  $\text{TiB}_2$  formation.

The three components heated in argon showed an endotherm at  $660^\circ\text{C}$  followed immediately by an exotherm starting at  $725^\circ\text{C}$ . The endotherm is due to the melting of aluminum, and the exotherm is due to reactants turning into products of  $\text{TiB}_2$  as supported by the XRD results (Figure 15).

## 4. Conclusions

This study has focused on the formation of a strong metal matrix bond containing submicron  $\text{TiB}_2$  particulates dispersed in an aluminum or titanium aluminide matrix. The primary source of heat for the formation of this bond would be derived from the generation of  $\text{TiB}_2$ . This investigation has demonstrated the important role that the gas phase surrounding the elemental metal powder compacts

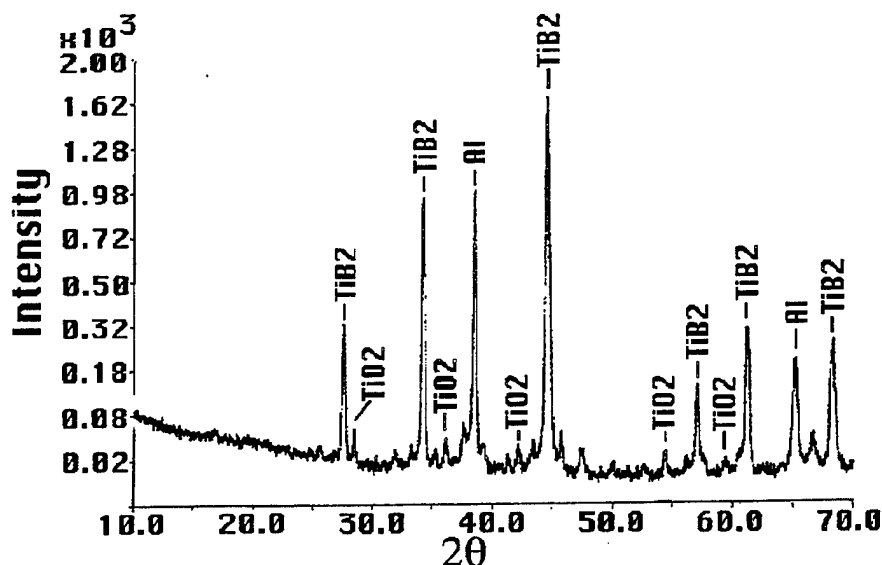


Figure 15. X-ray Diffraction of 50% by Weight Al + 50% (Ti + 2B) Reacted in Argon.

can play. For DTA/TGA experiments containing aluminum metal powder conducted in an argon atmosphere, the aluminum melting endotherm at  $660^{\circ}\text{C}$  is observed, followed by an exothermic reaction involving either titanium and boron or titanium and aluminum. It is believed that the molten aluminum metal dissolved a portion of the titanium and boron metal powders, and these two elements immediately react to form the desired  $\text{TiB}_2$  phase that generates the required heat to sustain the reaction. X-ray analysis confirmed the formation of  $\text{TiB}_2$  and the intermetallic phases of  $\text{TiAl}$  and  $\text{Ti}_3\text{Al}$ . In the case where just titanium and boron were reacted in argon, no exotherm was observed. The maximum temperature of the experiment ( $1,000^{\circ}\text{C}$ ) was not high enough to melt either titanium or boron. X-ray analysis of this material showed the major phase to be the unreacted titanium and minor phases of  $\text{TiB}$  and  $\text{TiB}_2$ , which were presumed to be formed by solid-state diffusion and, thus, did not initiate the SHS reaction.

In reactions involving air, all the pure metals and their mixtures exhibited strong exothermic reactions below the melting point of aluminum due to their oxidation. However, in the cases of metal mixtures, the heat generated by these reactions was greater than that expected for the oxidation process. It is believed that the excess heat produced by oxidation resulted in the localized melting

of the aluminum that then ignited the SHS reaction. X-ray analysis showed the metal oxides as well as the SHS products expected.

INTENTIONALLY LEFT BLANK.

## 5. References

1. U.S. National Research Council. STAR21: Strategic Technologies for the Army of the 21st Century. Washington, DC: National Academy Press, pp. 12-13, 159-169, 1992.
2. Montgomery, J., and O. Roopchand. *Journal of Metals*, pp. 45-47, May 1997.
3. Wickman, H., E. Chin, and R. Biederman. "Gamma Titanium Aluminide I, Diffusion Bonding of Titanium-Titanium Aluminide-Alumina Sandwich, TMS." Warrendale, PA, pp. 499-505, 1995.
4. Ohring, M. *The Materials Science of Thin Films*, 2nd edition, San Diego, CA: Academic Press, pp. 413-415, 1992.
5. Mills, N. *Plastics, Microstructure, Properties, Applications*, London, England: Edward Arnold Press, pp. 209-210, 1986.
6. Schwartz, M. "Ceramic Joining." ASM International, Materials Park, OH, pp. 75-87, 1990.
7. McCauley, J. *Ceram. Eng. Sci. Proc.*, vol. 11, no. 9-10, pp. 1137-1181, 1990.
8. Bowen, C., and B. Derby. *British Ceramic Transactions*, vol. 96, no. 1, pp. 25-31, 1997.
9. Wang, L., Z. Munir, and Y. Maximov. *J. of Mat. Sci.*, vol. 28, pp. 3693-3708, 1993.
10. Yi, H., and J. Moore. *J. of Mat. Sci.*, vol. 25, pp. 1159-1168, 1990.
11. Subrahmanyam, J., and M. Vijayakumar. *J. of Mat. Sci.*, vol. 27, no. 23, pp. 6249-6273, 1992.
12. Nagle, D., J. Brupbacher, and L. Christodoulou. U.S. Patent No. 4,774,052, 27 September 1988.
13. Moshier, W., D. Nagle, J. Brupbacher, and L. Christodoulou. U.S. Patent No. 4,738,389, 19 April 1988.
14. Christodoulou, L., and J. Brupbacher. *Materials Edge*, London, England, pp. 29-33, November 1990.
15. Lewis, D. *Metal Matrix Composites: Processing and Interfaces, In Situ Reinforcement of Metal Matrix Composites*, London, England: Academic Press, Inc., pp. 127-149, 1991.
16. Lide, D. *Handbook of Chemistry and Physics*, 71st edition, Boston, MA: CRC Press, Inc., sec. 4, pp. 113, 1990.

17. Moore, J., and H. Feng. *Progress in Materials Science, Combustion Synthesis of Advanced Materials: Part I. Reaction Parameters*, Tarrytown, NY: Elsevier Science Ltd., pp. 241-273, 1995.
18. Moore, J., and H. Feng. *Progress in Materials Science, Combustion Synthesis of Materials: Part II. Classification, Applications, and Modeling*, Tarrytown, NY: Elsevier Science Ltd., pp. 275-315, 1995.
19. Dodd, J., and K. Tonge. *Thermal Methods*, Chichester, England: John Wiley and Sons, Inc., pp. 110-139, 1987.
20. Mackenzie, R. *Differential Thermal Analysis I, Fundamental Aspects*, 2nd edition, London, England: Academic Press, Inc., pp. 38-59, 1970.

NO. OF COPIES	ORGANIZATION
2	DEFENSE TECHNICAL INFORMATION CENTER DTIC DDA 8725 JOHN J KINGMAN RD STE 0944 FT BELVOIR VA 22060-6218
1	HQDA DAMO FDQ D SCHMIDT 400 ARMY PENTAGON WASHINGTON DC 20310-0460
1	OSD OUSD(A&T)/ODDDR&E(R) R J TREW THE PENTAGON WASHINGTON DC 20301-7100
1	DPTY CG FOR RDE HQ US ARMY MATERIEL CMD AMCRD MG CALDWELL 5001 EISENHOWER AVE ALEXANDRIA VA 22333-0001
1	INST FOR ADVNCD TCHNLGY THE UNIV OF TEXAS AT AUSTIN PO BOX 202797 AUSTIN TX 78720-2797
1	DARPA B KASPAR 3701 N FAIRFAX DR ARLINGTON VA 22203-1714
1	NAVAL SURFACE WARFARE CTR CODE B07 J PENNELLA 17320 DAHLGREN RD BLDG 1470 RM 1101 DAHLGREN VA 22448-5100
1	US MILITARY ACADEMY MATH SCI CTR OF EXCELLENCE DEPT OF MATHEMATICAL SCI MAJ M D PHILLIPS THAYER HALL WEST POINT NY 10996-1786

NO. OF COPIES	ORGANIZATION
1	DIRECTOR US ARMY RESEARCH LAB AMSRL D R W WHALIN 2800 POWDER MILL RD ADELPHI MD 20783-1145
1	DIRECTOR US ARMY RESEARCH LAB AMSRL DD J J ROCCHIO 2800 POWDER MILL RD ADELPHI MD 20783-1145
1	DIRECTOR US ARMY RESEARCH LAB AMSRL CS AS (RECORDS MGMT) 2800 POWDER MILL RD ADELPHI MD 20783-1145
3	DIRECTOR US ARMY RESEARCH LAB AMSRL CI LL 2800 POWDER MILL RD ADELPHI MD 20783-1145
	<u>ABERDEEN PROVING GROUND</u>
4	DIR USARL AMSRL CI LP (305)

NO. OF  
COPIES ORGANIZATION

- |   |   |
|---|---|
| 1 | JOHNS HOPKINS UNIV<br>MATERIALS SCIENCE &<br>ENGRG DEPT<br>D NAGLE<br>3400 N CHARLES ST<br>BALTIMORE MD 21218 |
| 1 | PARATEK LLC<br>L CHIU<br>1202 TECHNOLOGY DR<br>SUITE C<br>ABERDEEN MD 21001                                   |



REPORT DOCUMENTATION PAGE			Form Approved OMB No. 0704-0188	
Public reporting burden for this collection of information is estimated to average 1 hour per response, including the time for reviewing instructions, searching existing data sources, gathering and maintaining the data needed, and completing and reviewing the collection of information. Send comments regarding this burden estimate or any other aspect of this collection of information, including suggestions for reducing this burden, to Washington Headquarters Services, Directorate for Information Operations and Reports, 1215 Jefferson Davis Highway, Suite 1204, Arlington, VA 22202-4302, and to the Office of Management and Budget, Paperwork Reduction Project(0704-0188), Washington, DC 20503.				
1. AGENCY USE ONLY (Leave blank)		2. REPORT DATE March 1999		3. REPORT TYPE AND DATES COVERED Final, Jun 97 - Jan 98
4. TITLE AND SUBTITLE  Thermal Analysis of Self-Propagating Reaction Joining Material			5. FUNDING NUMBERS  DAAL01-96-2-0047	
6. AUTHOR(S)  Luna H. Chiu, Dennis C. Nagle,* Daniel J. Snoha, and Kyu Cho				
7. PERFORMING ORGANIZATION NAME(S) AND ADDRESS(ES)  U.S. Army Research Laboratory ATTN: AMSRL-WM-MD Aberdeen Proving Ground, MD 21005-5069			8. PERFORMING ORGANIZATION REPORT NUMBER  ARL-TR-1906	
9. SPONSORING/MONITORING AGENCY NAMES(S) AND ADDRESS(ES)			10. SPONSORING/MONITORING AGENCY REPORT NUMBER	
11. SUPPLEMENTARY NOTES *Johns Hopkins University.				
12a. DISTRIBUTION/AVAILABILITY STATEMENT  Approved for public release; distribution is unlimited.			12b. DISTRIBUTION CODE	
13. ABSTRACT (Maximum 200 words)  This report focuses on the characterization of self-propagating high-temperature synthesis (SHS) reactions that occur in powder compacts containing titanium, boron, and aluminum. Interest in this powder system is based on the critical need to develop new joining techniques for bonding ceramics to metals. The exothermic reactions of particular interest in this study include those that generate TiB <sub>2</sub> , TiB, Ti <sub>3</sub> Al, and TiAl from their elemental powders. Data from differential thermal analysis, thermogravimetric analysis, and x-ray diffractometry are presented. These results demonstrate that the gas phase surrounding the SHS powders plays an important role in initiating the SHS reaction and in determining which reaction products will form in the final bond.				
14. SUBJECT TERMS  high-temperature synthesis, differential thermal analysis, thermogravimetric analysis, x-ray diffraction			15. NUMBER OF PAGES  28	
			16. PRICE CODE	
17. SECURITY CLASSIFICATION OF REPORT  UNCLASSIFIED	18. SECURITY CLASSIFICATION OF THIS PAGE  UNCLASSIFIED	19. SECURITY CLASSIFICATION OF ABSTRACT  UNCLASSIFIED	20. LIMITATION OF ABSTRACT  UL	

INTENTIONALLY LEFT BLANK.

## USER EVALUATION SHEET/CHANGE OF ADDRESS

This Laboratory undertakes a continuing effort to improve the quality of the reports it publishes. Your comments/answers to the items/questions below will aid us in our efforts.

1. ARL Report Number/Author ARL-TR-1906 (Chiu) Date of Report March 1999

2. Date Report Received \_\_\_\_\_

3. Does this report satisfy a need? (Comment on purpose, related project, or other area of interest for which the report will be used.) \_\_\_\_\_  
\_\_\_\_\_  
\_\_\_\_\_

4. Specifically, how is the report being used? (Information source, design data, procedure, source of ideas, etc.) \_\_\_\_\_  
\_\_\_\_\_  
\_\_\_\_\_

5. Has the information in this report led to any quantitative savings as far as man-hours or dollars saved, operating costs avoided, or efficiencies achieved, etc? If so, please elaborate. \_\_\_\_\_  
\_\_\_\_\_  
\_\_\_\_\_

6. General Comments. What do you think should be changed to improve future reports? (Indicate changes to organization, technical content, format, etc.) \_\_\_\_\_  
\_\_\_\_\_  
\_\_\_\_\_  
\_\_\_\_\_

CURRENT  
ADDRESS

\_\_\_\_\_  
Organization

\_\_\_\_\_  
Name

\_\_\_\_\_  
E-mail Name

\_\_\_\_\_  
Street or P.O. Box No.

\_\_\_\_\_  
City, State, Zip Code

7. If indicating a Change of Address or Address Correction, please provide the Current or Correct address above and the Old or Incorrect address below.

OLD  
ADDRESS

\_\_\_\_\_  
Organization

\_\_\_\_\_  
Name

\_\_\_\_\_  
Street or P.O. Box No.

\_\_\_\_\_  
City, State, Zip Code

(Remove this sheet, fold as indicated, tape closed, and mail.)  
(DO NOT STAPLE)